ORGANIC CHEMISTRY FRONTIERS

RESEARCH ARTICLE

View Article Online
View Journal | View Issue

Cite this: *Org. Chem. Front.*, 2025, **12**, 1754

Synthesis of a cross-chain bridging cryptand†‡

Takafumi Yashima, Ryoga Hori, Taisei Maruyama, Kohta Nakashima, Hiroki Fujihara, Masaya Naito, Shinobu Miyagawa and Yuji Tokunaga *

Received 12th December 2024,
Accepted 9th January 2025

DOI: 10.1039/d4qo02330g

rsc.li/frontiers-organic

We present two methodologies for synthesizing cross-chain bridging cryptand **1** that incorporates tri- and tetra(ethylene glycol) linkers (methods B and C). Method B involves the synthesis through the intramolecular cross-linking of C_2-symmetric crown ether **3**. While this method does not substantially reduce the lengthy reaction steps compared to the previous approach, it improves the overall yield of cryptand **1a** containing three tri(ethylene glycol) linkers and allows for the creation of a new form of a cross-chain bridging cryptand **1c** with one distinct and two identical linkers. However, method C entails a synthesis accomplished through a triple-linking reaction in a single step. This method offered a streamlined synthesis of cryptand **1**. The crucial triple linking reaction produced cross-chain bridging cryptand **1** as the major isomer and the corresponding linear regioisomer **6** as the minor isomer. Moreover, we observed the interconversion of enantiomers of cryptand **1c**, which contains a 28-membered macrocycle, under chiral high-performance liquid chromatographic (HPLC) analytical conditions (with a half-life of 20.7 min at room temperature). Finally, X-ray crystallography confirmed the cross-chain bridging structure in the two chemically equivalent chains in the solid state of cryptand **1a**.

Introduction

Many molecularly chiral architectures have been developed from unique structural systems that lack classical chiral elements.[1] These include increasingly complex molecular arrangements, such as calixarene host families,[2] their analogs,[3–7] helicenes,[8] other distorted aromatics,[8c,d,9–12] Möbius strips,[13] and others.[8d,14,15] These inherently chiral architectures are structurally intriguing, and their chiroptical properties have been extensively studied.[8b,16–20]

The development of a cross-chain bridging structure represents an intriguing approach for inducing molecular chirality in the absence of asymmetric centers. Figure-of-eights are representative examples of creating such chiral systems.[8d,21,22] For a chiral figure-of-eight structure to be effective, it must incorporate rigid functional groups to inhibit the interconversion of its enantiomers. Walba and colleagues have successfully synthesized a chiral Möbius strip featuring a cross-chain bridging arrangement, demonstrating the induction of chirality without requiring rigid linkers.[23] Currently, molecular knots and links with multiple and intricately entangled structures have been synthesized through transition metal templating and/or thermodynamically controlled methodologies,[24] with one such system being used as an asymmetric catalyst in organic reactions.[25]

In a previous work, we synthesized a cross-chain bridging cryptand **1** bearing three oligo(ethylene glycol) linkers (Fig. 1).[26] The cryptand exhibits C_2 symmetry, and its cross-chain bridging structure is formed through triple linking at different positions of two benzene moieties, with two of the three cross-chain linkers being chemically equivalent. Cryptand **1a**, which contains three tri(ethylene glycol) linkers and a 25-membered macrocycle, demonstrates molecular chirality. However, the conversion of the enantiomers of the larger cryptand **1b**, which features long linkers, occurred at room temperature (Fig. S1‡) owing to the large 31-membered macrocycle in **1b** failing to sufficiently inhibit the flipping of the benzoate moiety. Consequently, this type of cross-chain bridging cryptand can act as both chiral and dynamic chiral hosts, allowing for variation in the size of the macrocycles.

In a previous study, the cross-chain bridging cryptand was synthesized through the intramolecular cross-linking of the unsymmetric crown ether **2** (Fig. 1, method A). The primary advantage of method A is that it yields cryptand **1** as a single product when the intramolecular cross-linking reaction is performed. However, this method requires extensive synthetic steps, resulting in relatively low total yields of the cryptand, particularly owing to the low yield associated with the synthesis of crown ether **2**. Additionally, this approach is limited to the production of cross-chain bridging cryptands featuring three identical linkers for creating C_2-symmetric cryptands.

Department of Materials Science and Engineering, Faculty of Engineering, University of Fukui, Bunkyo, Fukui 910-8507, Japan. E-mail: tokunaga@u-fukui.ac.jp

†Dedicated to Professor Dr Frank Würthner on the occasion of his 60th birthday.

‡Electronic supplementary information (ESI) available: Synthetic procedures, analytical data, and a cif file for the single-crystal X-ray analysis. CCDC 2392777. For ESI and crystallographic data in CIF or other electronic format see DOI: https://doi.org/10.1039/d4qo02330g

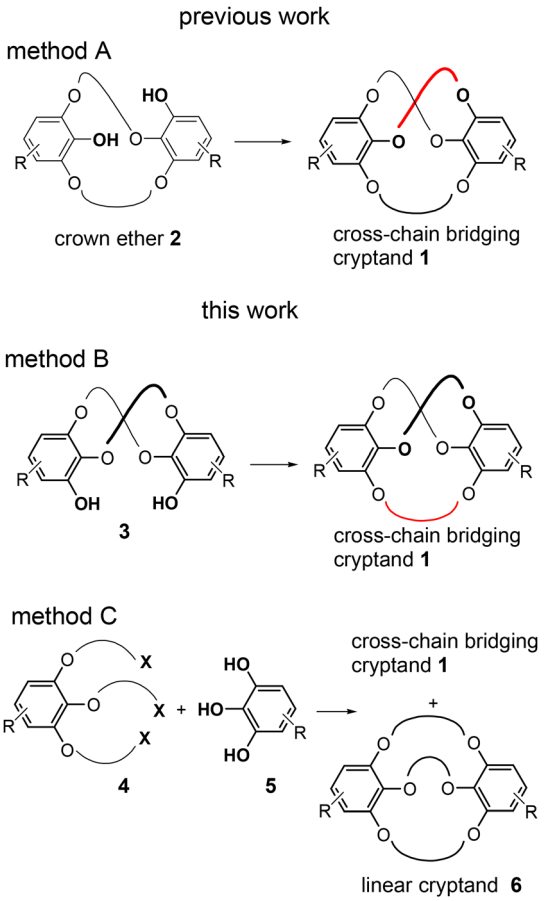

Fig. 1 Synthetic strategies for cross-chain bridging cryptand **1**.

Here, we present two new methodologies for the synthesis of cross-chain bridging cryptand **1** (Fig. 1, methods B and C).[27] In method B, the intramolecular cross-linking of C_2-symmetric crown ethers **3** is a key step, while method C involves performing the triple linking reaction in a single step. Although method B does not considerably reduce the number of lengthy reaction steps, it increases the synthetic yield of the small cryptand. Furthermore, this method allows for the incorporation of a distinct linker different from the other two, enabling the synthesis of a new type of cross-chain bridging cryptand featuring two types of linkers. However, method C offers a short-step synthesis of cryptand **1**, with the final triple linking step producing cross-chain bridging cryptand **1** as the major isomer alongside the corresponding linear regioisomer **6**. Additionally, we confirmed through X-ray crystallography that cryptand **1a**, bearing three tri(ethylene glycol) units as linkers, exhibits a cross-chain bridging structure formed by two chemically equivalent linkers.

Results and discussion

Synthesis of cryptand 1 by linking the C_2-symmetric crown ethers 3 (method B)

We used 3-*O*-benzyl ethyl gallate (**7**)[26] as the starting material for synthesizing the C_2-symmetric crown ethers **3** (Scheme 1).

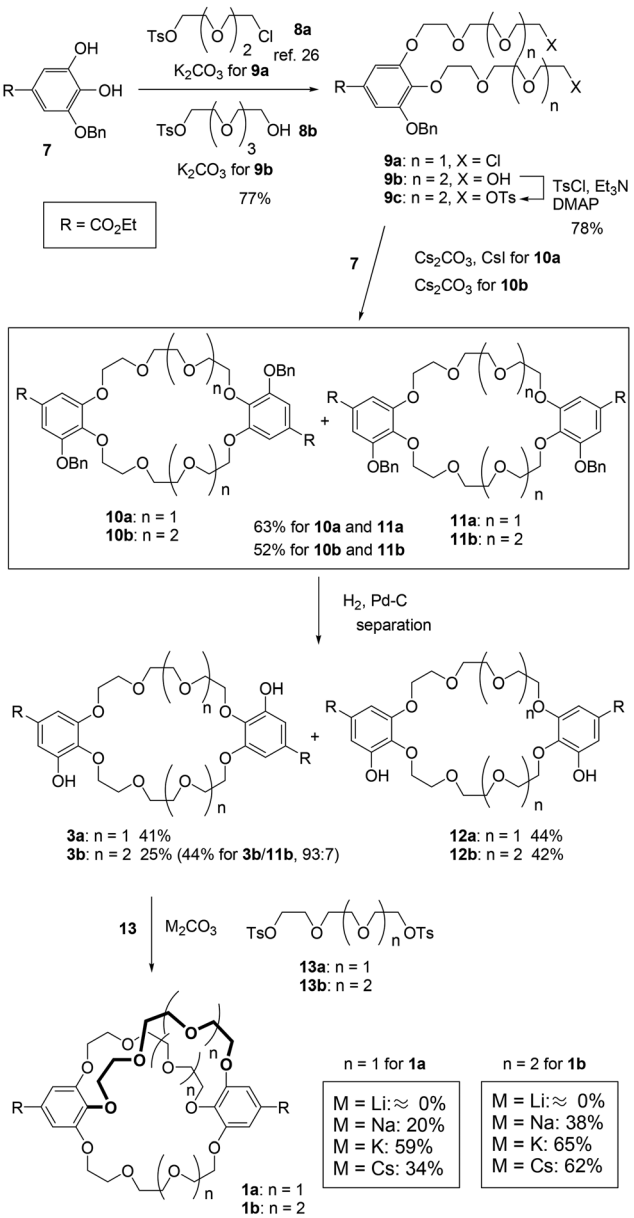

Scheme 1 Method B: synthesis of cross-chain bridging cryptand **1**.

Alkylation of compound **7** and the corresponding tosylates **8**, which contain tri- and tetra(ethylene glycol) units, produced the oligoethers **9**. To synthesize larger crown ethers (**10b** and **11b**), diol **9b** was converted into ditosylate **9c**. Macrocyclization of either dichloride **9a** or ditosylate **9c** with ethyl gallate **7** resulted in a 1 : 1 mixture of C_2-symmetric crown ethers **10** and σ-symmetric crown ethers **11**, obtained in moderate yields. These mixtures were subsequently converted into the corresponding deprotected crown ethers **3** and **12** as additional mixtures. C_2-symmetric and σ-symmetric small crown ethers **3a** and **12a** were successfully isolated through chromatographic separation. The ^{1}H NMR spectra of crown ethers **3a** and **12a** indicated their symmetric structures. Specifically, the spectrum of **12a**, which features two sets of chemically equivalent

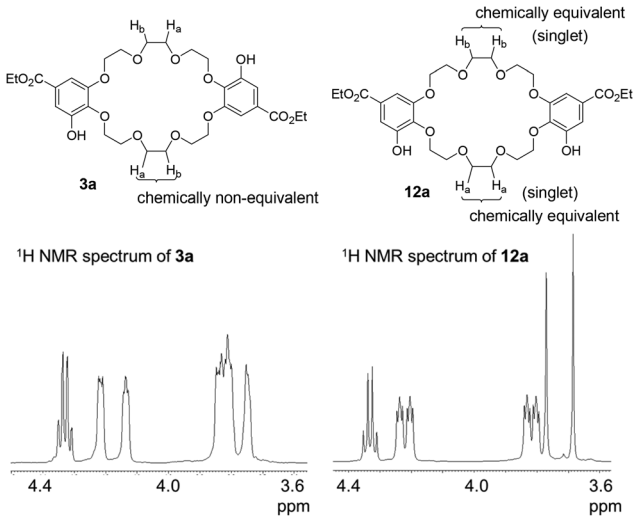

Fig. 2 Structures and ^{1}H NMR spectra (600 MHz, $CDCl_3$) of crown ethers **3a** and **12a**.

protons in the ethylene glycol units (Fig. 2), showed two singlet signals for the ethylene glycol protons at 3.77 and 3.69 ppm. In contrast, the ^{1}H NMR spectrum of **3a** did not exhibit any singlet signals from the ethylene glycol units. The separation of crown ethers **3b** and **12b**, which contain long linkers, was achieved through crystallization. After the deprotection of the benzyl groups in the mixture of **10b** and **11b**, the crude product was treated with MeOH, affording a solid that consisted of a 93 : 7 mixture of **3b** and **12b** in 44% yield. Further washing of this mixture with EtOH resulted in the isolation of C_2-symmetric crown ether **3b** as a single product with a yield of 25%. σ-Symmetric crown ether **12b** was obtained as a solid from the first filtrate after treatment with ^{i}PrOH. At this stage, the structures of the isomers were not elucidated through ^{1}H NMR spectroscopy. Finally, we established their structures following the conversion of **3b** and **12b** into the cross-chain bridging and linear cryptands **1b** and **6b**, respectively (as described below).

The synthesis of the cross-chain bridging cryptand **1** from **3** and the corresponding ditosylate **13** was investigated using four carbonates as bases and templates (Scheme 1). K_2CO_3 proved to be the most effective base for producing the small cross-chain bridging [4.4.4]cryptand **1a** with a yield of 59%.[28] The cross-linking of crown ether **3b** led to the formation of the large [5.5.5]cryptand **1b**, achieved using K_2CO_3 and Cs_2CO_3 with a good yield. To evaluate the products of the cross-linking reactions, the crude products were analyzed by gel permeation chromatography (GPC) (Fig. S2 and S3‡).

When Li_2CO_3 was used as a base for the synthesis of **1**, only crown ethers **3** were recovered because the combination of the crown ethers and the carbonate salt resulted in the formation of an insoluble complex(es). After the workup of the reaction between **3b** and **13b**, only the peak corresponding to **3b** was present in the chromatogram (Fig. S3a for **3b**‡). In contrast, when using Na_2CO_3, the peaks of cryptand **1** appeared prominently alongside other distinct peaks in the chromatograms. For the synthesis of the small [4.4.4]cryptand **1a**, a non-negligible peak was observed before the peak for **1a** with both K_2CO_3 and Cs_2CO_3. The cyclization of two molecules of crown ether **3a** and ditosylate **13a** likely yielded the larger macrocycle.[29] Conversely, peaks for the large [5.5.5]cryptand **1b** were detected in the chromatograms when K_2CO_3 and Cs_2CO_3 were used. The template effect of the potassium ion is more effective than that of the cesium ion for synthesizing the small cryptand **1a**, while both potassium and cesium ions may serve as effective templates for the synthesis of the large cryptand **1b**. Upon purification of the cryptand using GPC, we confirmed that the ^{1}H NMR spectra matched those previously reported.[26]

Synthesis of the cross-chain bridging cryptand 1c possessing two different linkers

Next, we synthesized [5.5.4]cryptand **1c**, which contains two tetra(ethylene glycol) linkers and one tri(ethylene glycol) linker, to demonstrate that method B allows the construction of a cryptand with two different types of linkers (Scheme 2). The macrocyclization reaction involving the large C_2-symmetric crown ether **3b** and tri(ethylene glycol) ditosylate **13a**, using K_2CO_3 and Cs_2CO_3, yielded [5.5.4]cryptand **1c** in 52% yield under both conditions.

The mass spectrum (MALDI) of cryptand **1c** showed a peak at m/z 849.3499 (calcd 849.3515), which corresponds to a complex with the sodium cation ($[M + Na]^+$) (Fig. S10‡). The NMR spectra of **1c** in C_6D_6 indicate that the cryptand possesses a C_2 symmetric structure. In the ^{13}C NMR spectrum of **1c**, ten carbon signals from the ethylene glycol units were observed at 73.1, 71.4, 71.3, 71.1, 71.0, 70.9, 69.8, 69.7, 69.6, and 69.1 ppm; one signal appeared to overlap, although eleven signals would be expected theoretically (Fig. S5‡). In the ^{1}H NMR spectrum, several signals overlapped, yet many proton signals from the ethylene glycol units were split into two (Fig. 3 and S4‡). This splitting is attributed to the desymmetrization of the crown ether moiety in the cryptand, caused by cross-chain bridging. These observations suggest that the interconversion of the enantiomers of the 28-membered **1c** does not proceed or occurs slowly on the NMR spectroscopic time scale, as indicated by the similar ^{1}H NMR spectral features of the previously reported 25-membered [4.4.4]cryptand **1a**.[26] The interconversion likely involves the rotation of the benzoate moiety (Fig. S1‡), but the 28-membered crown macro-

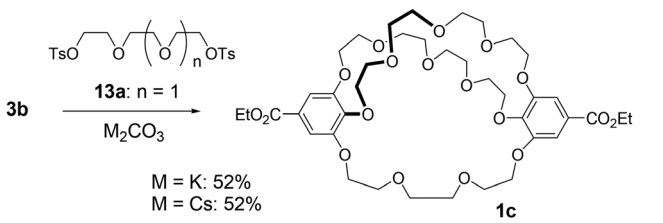

Scheme 2 Method B: synthesis of cross-chain bridging cryptand **1c**.

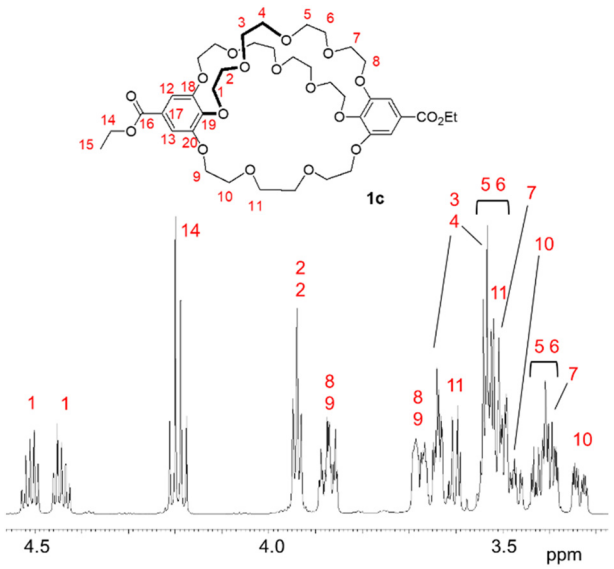

Fig. 3 Partial ^{1}H NMR spectrum (600 MHz, C_6D_6) of cryptand **1c**.

cycle lacks sufficient space for the rotation of ethyl benzoate in the NMR spectroscopic time scale at room temperature. The proton and carbon signals of **1c** were assigned using 2D NMR spectroscopy (Fig. S6–S9‡).

Synthesis of linear cryptand 6 by linking σ-symmetric crown ethers 12

To synthesize linear cryptand **6** before method C and to confirm the structures of the crown ethers (**3b** and **12b**), which could not be determined by NMR spectroscopy (as described above), we linked the σ-symmetric crown ethers **12** with the ditosylates **13** using Cs_2CO_3 as a base (Scheme 3).

The mass spectra (MALDI) of the small [4.4.4]cryptand **6a** (derived from **12a** and **13a**) and the large [5.5.5]cryptand **6b** (derived from **12b** and **13b**) exhibit peaks at *m*/*z* 761.2994 (calcd 761.2991) and 893.3775 (calcd 893.3778), respectively, corresponding to the sodium ion complexes ($[M + Na]^+$) (Fig. S14 for **6a** and Fig. S18 for **6b**‡). The ^{1}H NMR spectra of both cryptands were in line with the highly symmetric structures of the linear cryptand. For instance, six sets of signals for ethylene glycol protons were identified at 4.17 (8H), 4.14 (4H), 3.96 (4H), 3.89 (8H), 3.80 (8H), and 3.79 ppm (4H).

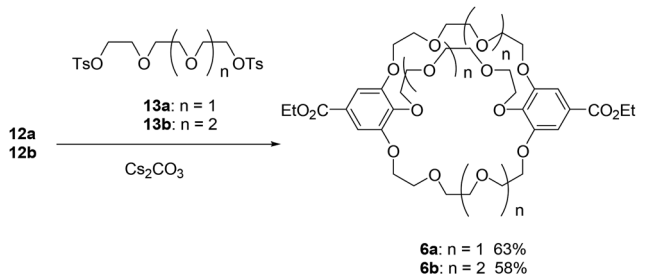

Scheme 3 Synthesis of linear cryptand **6**.

Additionally, two singlet signals (3.80 and 3.79 ppm) were observed in the ^{1}H NMR spectrum of **6a** (Fig. S11‡). The signal pattern and the integration confirmed the structure of linear cryptand **6a**. Likewise, the ^{1}H NMR spectrum of **6b** also confirmed the structure of the linear cryptand (Fig. S15‡). All proton signals were assigned through 2D NMR experiments performed on linear cryptand **6** (Fig. S12 and S13 for **6a** and Fig. S16 and S17 for **6b**‡).

The isomeric structures of the crown ethers (**3** and **12**) and the cryptands (**1** and **6**) were confirmed through chemical conversion and NMR analysis of the products.

Short-step synthesis of cryptand 1 by triple linking in one step (method C)

First, we synthesized trichloride **14** through the alkylation of ethyl gallate (**5**) and chlorotosylate, which was essential for the key triple linking reaction (Scheme 4). However, the triple linking of **14** with ethyl gallate (**5**) was inconsistent, preventing the successful production of cryptands **1a** and **6a** owing to the generation of insoluble complexes during the process. To enhance the solubility of the substrates and intermediates, we then produced tritosylates **4** for the triple linking reaction by alkylating ethyl gallate (**5**) with the monotosylate of tri- and tetra(ethylene glycol) and subsequently tosylating the triols **15**. As mentioned earlier, potassium and cesium ions act as efficient templates during the final linking steps (the conversion of crown ethers **3** to cryptands **1**) in method B. The triple linkage of tritosylates **4** with ethyl gallate (**5**) was performed using K_2CO_3 and Cs_2CO_3 as bases and templates, respectively. Following GPC and high-performance liquid chromatographic

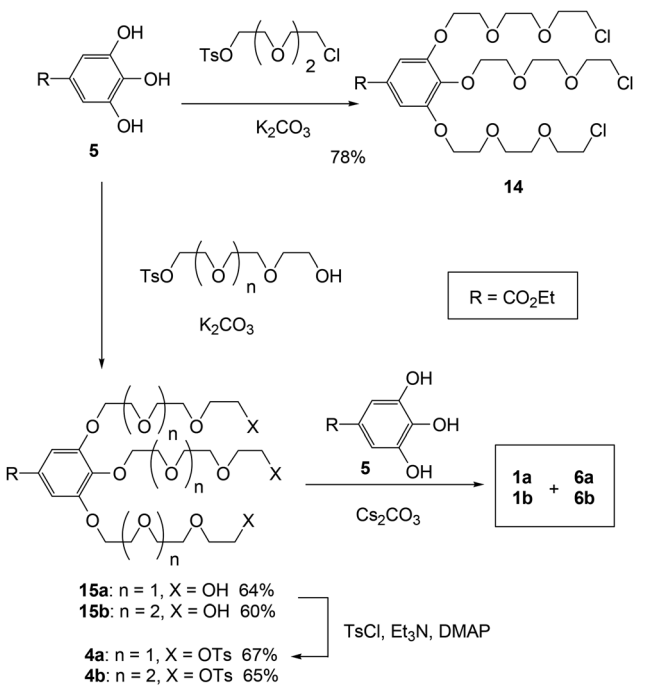

Scheme 4 Method C: synthesis of cross-chain bridging cryptand **1** and linear cryptand **6**.

(HPLC) separation, we successfully isolated cross-chain and linear cryptands **1** and **6**. The ^{1}H NMR spectra of all isolated cryptands (**1** and **6**) matched those of the products obtained through the abovementioned methods. The isolated yields for both the cross-chain bridging and linear cryptands from the triple-linking reactions ranged from 24% to 32% across all experiments (Table 1). Notably, the yields of cross-chain bridging cryptand **1** consistently surpassed those of linear cryptand **6**, and K_2CO_3 provided slightly higher yields for both cryptands compared to Cs_2CO_3.

The detailed processes of the triple linking reaction between tosylate **4** and ethyl gallate **5** are shown in Fig. 4. In the initial linking step, the hydroxy group at the 4-position of ethyl gallate primarily undergoes deprotonation owing to the electron-withdrawing effect of the ethoxy carbonyl group. Consequently, the phenoxide anion is likely to statistically attack the tosyloxy alkyl groups located at the 3- (5-) and 4-positions in tosylate **4**, resulting in a 2 : 1 mixture of intermediates **A** and **B**. The subsequent intramolecular linking of intermediate **A** is expected to yield the cross-chain bridging cryptand **1** through intermediates **C** and **D**, which correspond to the key precursors from methods B and A, respectively. In contrast, only linear cryptand **6** is expected to be formed from the second and third intramolecular linking of intermediate **B** *via* intermediate **E**. Consequently, the triple linking reaction may statistically yield a 2 : 1 mixture of the cross-chain bridging cryptand **1** and linear cryptand **6**, assuming that only the 4-hydroxy group of ethyl gallate is deprotonated and that the second and third linking reactions occur equally. However, the observed experimental selectivity of the triple linking reactions was lower than this statistical ratio (2 : 1). Previous studies on each linking reaction involving the analogs of the intermediates (methods A and B) indicated that the macrocyclization of the **A**-analog produced the **D**-analog in a poor yield (method A). As a result, the proportion of linear cryptand **6** may increase relative to the cross-chain product. Additionally, a minor first alkylation at the 3-hydroxy group of ethyl gallate could further enhance the ratio of linear cryptand **6**. The detailed minor processes of the triple linking reaction are provided in the ESI (Fig. S19‡).

The isolated yields of both cryptands may align with the yields observed from the two macrocyclization reactions of method B (first macrocyclization: 63% and 52% yields for the synthesis of 1 : 1 mixtures of crown ethers **10** and **11a** in the presence of Cs_2CO_3; second macrocyclization: 34–65% yields for the synthesis of cryptands **1** and **6** in the presence of K_2CO_3 or Cs_2CO_3). The overall isolated yields (24–32%) are a result of the moderate yields achieved in the two macrocyclization reactions.

Table 1 Method C. Isolated yields of cryptands **1** and **6** obtained through the triple-linking reaction

	K_2CO_3 isolated yield	Cs_2CO_3 isolated yield
[4.4.4]cryptand	**1a**: 17%	**1a**: 15%
	6a: 15%	**6a**: 10%
[5.5.5]cryptand	**1b**: 17%	**1b**: 15%
	6b: 13%	**6b**: 9%

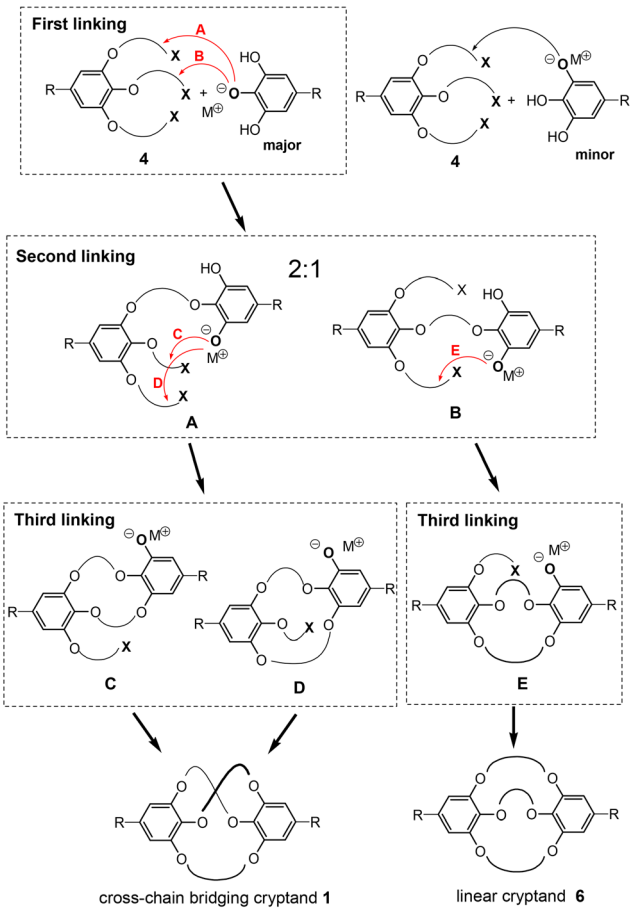

Fig. 4 Key steps in the triple-linking reaction between tosylate **15** and ethyl gallate.

Total yields and steps for the synthesis of the cross-chain bridging cryptand 1 using three methods

Table 2 shows the total yields and number of steps for the three methods used in the synthesis of cross-chain bridging cryptand **1**. The new methods (B and C) considerably enhanced the yields for synthesizing the small cross-chain bridging cryptand **1a**, with method B showing the most improvement. Conversely, method A yields the best results for preparing the larger cryptand **1b**. Though method C allows for

Table 2 Total yields and steps for synthesizing cross-chain bridging cryptand **1** *via* three methods

	Method A[a]	Method B	Method C
[4.4.4]cryptand	3.6 and 3.0%	**9.5%**	7.3%
1a	10 steps[b]	9 steps	**4 steps**
[5.5.5]cryptand	**7.6%**	4.3%	6.6%
1b	11 steps	10 steps	**4 steps**

[a] Ref. 26. [b] Method A includes two approaches for cryptand **1a**.

a shorter step-synthesis of cryptand **1**, it requires HPLC and GPC for the isolation of each cryptand.

Chiral HPLC analysis of cryptand 1c: observation of racemization

The 25-membered cryptand **1a** is chiral, whereas the racemization of the 31-membered cryptand **1b** occurred at room temperature under NMR spectroscopic conditions. As mentioned above, the interconversion of the 28-membered cryptand **1c** was not detected by NMR spectroscopy. Subsequently, we investigated the chiral HPLC separation of the enantiomers of **1c** using CHIRALPAK IG-3 as the stationary phase (Fig. S20‡). The chromatogram displayed the typical sharp peaks for both enantiomers of **1c**, along with a plateau peak located between these peaks, indicating that the racemization of **1c** was occurring slowly under the HPLC conditions. Additionally, changes in flow rate affected the ratio of the peak areas, which was dependent on the retention time. The two usual peaks and the plateau peak were attributed to the nonracemized and racemized forms of **1c**, respectively. A plot of ln[(peak area of enantiomers)/(total area)] *versus* time (t) produced a straight line, allowing us to determine a racemization rate constant k of 5.57 $\times 10^{-4}$ (s^{-1}) and a half-life (τ) of 20.7 min at room temperature from the first-order plot (Fig. 5).[30,31] While the racemization reaction is too rapid to isolate both enantiomers of **1c**, increasing the steric bulk of the benzoate groups in **1c** is likely to inhibit racemization because this reaction may occur through the rotation of the benzoate moiety.

In this study, considering the racemization rate of the cryptand, we only show the ring member of macrocycles. However, the length of the crossing-chain linkage should affect the rate because the length influences the flexibility and precise size of the macrocycle even though the ring member is identical. Further experimental studies should be needed to elucidate the effects of the cross-chain linkage on the racemization rate.

Crystal structure of the cross-chain bridging cryptand 1a

In our previous work, we successfully crystallized a 1 : 1 complex of the (−)-[4.4.4]cryptand **1a** with NH_4PF_6.[26] X-ray crystallography analysis indicated that two chemically equivalent tri(ethylene glycol) linkers were entangled in the solid, and the absolute configuration of the complex was established. In this study, we obtained a single crystal for analysis by recrystallizing (±)-[4.4.4]cryptand **1a** in the absence of any additional species, using slow evaporation of a 1 : 1 acetone/hexane mixture at room temperature. The crystal structure revealed that **1a** adopted an approximately C_2-symmetric conformation, with two benzene rings arranged in parallel (Fig. 6 and S21, Table S1‡). As expected, the two chemically equivalent tri(ethylene glycol) chains became cross-linked with each other, a structure resembling that of the (−)-**1a** and NH_4PF_6 complex in the solid state. A pair of enantiomers assembled to form a crystal lattice featuring six CH–O intermolecular interactions between the CH groups and the oxygen in the ethylene glycol chains, alongside four CH–π intermolecular interactions between the ethylene glycol CH groups and the phenyl groups (Fig. S21a‡). One enantiomer aligned along the a axis, resulting in a hetero-columnar crystal, with two crown cavities of **1a** oriented perpendicularly along the a axis (Fig. S21b‡).

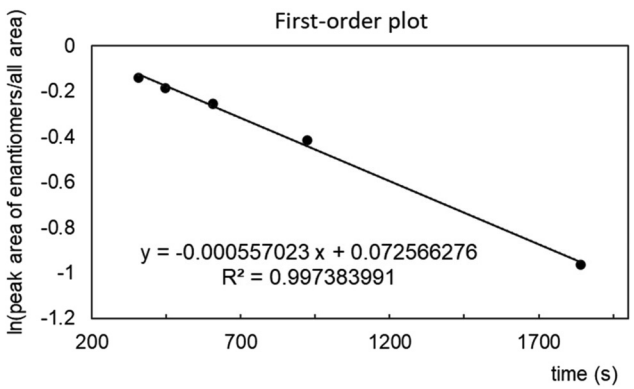

Fig. 5 First-order plot depicting the racemization of cryptand **1c** under HPLC conditions.

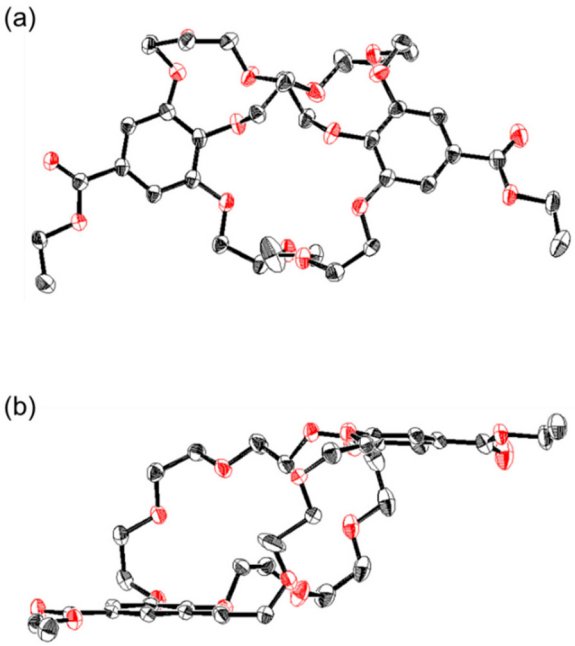

Fig. 6 ORTEP representation of the solid-state structure of cryptand **1a**. (a) Overhead view and (b) side view. Thermal ellipsoids are shown at the 50% probability level. For clarity, hydrogen atoms and disordered oxyethylene chains are omitted. Black: carbon; red: oxygen.

Conclusions

We explored two new methodologies (methods B and C) for synthesizing cryptand **1**. In method B, we produced the cross-chain bridging cryptand **1** through the linkage of C_2-symmetric crown ethers **3**. This approach increased the overall yield and reduced the number of steps for synthesizing [4.4.4]cryptand **1a**, using K_2CO_3 as a base and template for the final cross-

linking step. However, the total yield of [5.5.5]cryptand **1b** did not surpass that of the earlier methodology (method A). Notably, method B allowed the synthesis of a new type of cross-chain bridging cryptand **1c**, which incorporates two tetra(ethylene glycol) linkers and one tri(ethylene glycol) linker. This is a new type of cross-chain bridging cryptand featuring various linkers and a C_2-symmetric structure. Furthermore, the isomeric σ-symmetric crown ethers generated during the initial macrocyclization were transformed into linear cryptand **6** to elucidate the structures of the crown ethers. The triple linking method was investigated for synthesizing cross-chain bridging cryptand **1** from tritosylate **4** and ethyl gallate (method C). The final triple linking step predominantly yielded cross-chain bridging cryptand **1** as the major isomer, while the corresponding linear regioisomer **6** appeared as the minor isomer. Both cross-chain bridging cryptand **1** and linear cryptand **6** could be isolated using GPC and HPLC separation techniques. This methodology could considerably reduce the total number of synthetic steps required for preparing cryptand **1**. Chiral HPLC analysis of cryptand **1c**, which features a 28-membered macrocycle, demonstrated the interconversion of enantiomers, with a half-life of 20.7 min at room temperature. Finally, X-ray crystal analysis confirmed the cross-chain bridging structure of the chemically equivalent chains in cryptand **1a**.

Author contributions

T. Y., R. H., T. M., K. N., and H. F.: investigation, data curation, and formal analysis, M. N.: investigation, data curation, and analysis of X-ray crystallography, S. M.: investigation, data curation, and analysis of mass spectrometry, and Y. T.: conceptualization, supervision, and writing – original draft.

Data availability

The data that support the findings of this study are available in the ESI‡ of this article.

Conflicts of interest

There are no conflicts to declare.

Acknowledgements

This study was supported by JSPS KAKENHI [JP20K05461 (YT) and JP24K08392 (YT)] and Izumi Science and Technology Foundation.

References

1 A. Szumna, Inherently Chiral Concave Molecules—from Synthesis to Applications, *Chem. Soc. Rev.*, 2010, **39**, 4274–4285.
2 (*a*) V. Böhmer, D. Kraft and M. Tabatabai, Inherently Chiral Calixarenes, *J. Inclusion Phenom. Mol. Recognit. Chem.*, 1994, **19**, 17–39; (*b*) Y.-S. Zheng and J. Luo, Inherently Chiral Calixarenes: A Decade's Review, *J. Inclusion Phenom. Mol. Recognit. Chem.*, 2011, **71**, 35–56; (*c*) G. E. Arnott, Inherently Chiral Calixarenes: Synthesis and Applications, *Chem. – Eur. J.*, 2018, **24**, 1744–1754.
3 T. Ogoshi, T. Yamagishi and Y. Nakamoto, Pillar-Shaped Macrocyclic Hosts Pillar[*n*]arenes: New Key Players for Supramolecular Chemistry, *Chem. Rev.*, 2016, **116**, 7937–8002.
4 X.-N. Han, Y. Han and C.-F. Chen, Pagoda[4]arene and *i*-Pagoda[4]arene, *J. Am. Chem. Soc.*, 2020, **142**, 8262–8269.
5 G.-W. Zhang, P.-F. Li, Z. Meng, H.-X. Wang, Y. Han and C.-F. Chen, Triptycene-Based Chiral Macrocyclic Hosts for Highly Enantioselective Recognition of Chiral Guests Containing a Trimethylamino Group, *Angew. Chem., Int. Ed.*, 2016, **55**, 5304–5308.
6 A. Collet, Cyclotriveratrylenes and Cryptophanes, *Tetrahedron*, 1987, **43**, 5725–5759.
7 T. Brotin and J.-P. Dutasta, Cryptophanes and Their Complexes–Present and Future, *Chem. Rev.*, 2009, **109**, 88–130.
8 Selected reviews of helicenes: (*a*) Y. Shen and C. F. Chen, Helicenes: Synthesis and Applications, *Chem. Rev.*, 2012, **112**, 1463–1535; (*b*) K. Dhbaibi, L. Favereau and J. Crassous, Enantioenriched Helicenes and Helicenoids Containing Main-Group Elements (B, Si, N, P), *Chem. Rev.*, 2019, **119**, 8846–8953; (*c*) H. V. Anderson, N. D. Gois and W. A. Chalifoux, New Advances in Chiral Nanographene Chemistry, *Org. Chem. Front.*, 2023, **10**, 4167–4197; (*d*) M. Rickhaus, M. Mayor and M. Juricek, Strain-Induced Helical Chirality in Polyaromatic Systems, *Chem. Soc. Rev.*, 2016, **45**, 1542–1556.
9 Y. Segawa, H. Ito and K. Itami, Structurally Uniform and Atomically Precise Carbon Nanostructures, *Nat. Rev. Mater.*, 2016, **1**, 15002.
10 M. Saito, H. Shinokubo and H. Sakurai, Figuration of Bowl-Shaped π-Conjugated Molecules: Properties and Functions, *Mater. Chem. Front.*, 2018, **2**, 635–661.
11 I. R. Marquez, S. Castro-Fernandez, A. Millan and A. G. Campana, Synthesis of Distorted Nanographenes Containing Seven- and Eight-Membered Carbocycles, *Chem. Commun.*, 2018, **54**, 6705–6718.
12 Y. Zhang, S. H. Pun and Q. Miao, The Scholl Reaction as a Powerful Tool for Synthesis of Curved Polycyclic Aromatics, *Chem. Rev.*, 2022, **122**, 14554–14593.
13 Selected reviews and examples of Möbius strips: (*a*) R. Herges, Topology in Chemistry: Designing Möbius Molecules, *Chem. Rev.*, 2006, **106**, 4820–4842; (*b*) S. Nishigaki, Y. Shibata, A. Nakajima, H. Okajima, Y. Masumoto, T. Osawa, A. Muranaka, H. Sugiyama, A. Horikawa, H. Uekusa, H. Koshino, M. Uchiyama, A. Sakamoto and K. Tanaka, Synthesis of Belt- and Möbius-Shaped Cycloparaphenylenes by Rhodium-Catalyzed Alkyne Cyclotrimerization, *J. Am. Chem. Soc.*, 2019, **141**,

14955–14960; (*c*) J. Yuan, Y. Song, X. Li, J. Xie, S. Dong and K. Zhu, A Tubular Belt and a Möbius Strip with Dynamic Joints: Synthesis, Structure, and Host–Guest Chemistry, *Org. Lett.*, 2021, **23**, 9554–9558; (*d*) S. Wang, J. Yuan, J. Xie, Z. Lu, L. Jiang, Y. Mu, Y. Huo, Y. Tsuchido and K. Zhu, Sulphur-Embedded Hydrocarbon Belts: Synthesis, Structure and Redox Chemistry of Cyclothianthrenes, *Angew. Chem., Int. Ed.*, 2021, **60**, 18443–18447; (*e*) Y. Segawa, T. Watanabe, K. Yamanoue, M. Kuwayama, K. Watanabe, J. Pirillo, Y. Hijikata and K. Itami, Synthesis of a Möbius Carbon Nanobelt, *Nat. Synth.*, 2022, **1**, 535–541; (*f*) B. Yao, X. Liu, T. Guo, H. Sun and W. Wang, Molecular Möbius Strips: Twist for a Bright Future, *Org. Chem. Front.*, 2022, **9**, 4171–4177.

14 Y. Segawa, A. Yagi, K. Matsui and K. Itami, Design and Synthesis of Carbon Nanotube Segments, *Angew. Chem., Int. Ed.*, 2016, **55**, 5136–5158.

15 S. Sato, A. Yoshii, S. Takahashi, S. Furumi, M. Takeuchi and H. Isobe, Chiral Intertwined Spirals and Magnetic Transition Dipole Moments Dictated by Cylinder Helicity, *Proc. Natl. Acad. Sci. U. S. A.*, 2017, **114**, 13097–13101.

16 H. Lu and N. Kobayashi, Optically Active Porphyrin and Phthalocyanine Systems, *Chem. Rev.*, 2016, **116**, 6184–6261.

17 H. Tanaka, Y. Inoue and T. Mori, Circularly Polarized Luminescence and Circular Dichroisms in Small Organic Molecules: Correlation between Excitation and Emission Dissymmetry Factors, *ChemPhotoChem*, 2018, **2**, 386–402.

18 T. Mori, Chiroptical Properties of Symmetric Double, Triple, and Multiple Helicenes, *Chem. Rev.*, 2021, **121**, 2373–2412.

19 M. Hasegawa, Y. Nojima and Y. Mazaki, Circularly Polarized Luminescence in Chiral π-Conjugated Macrocycles, *ChemPhotoChem*, 2021, **5**, 1042–1058.

20 Y. Zhang, J. Guan, L. Luo, X. Han, J. Wang, Y. Zheng and J. Xu, Chiral Twisted Molecular Carbons: Synthesis, Properties, and Applications, *Interdiscip. Mater.*, 2024, **3**, 453–479.

21 Selected reviews and examples of figure-of-eight: (*a*) M. Stępień, N. Sprutta and L. Latos-Grażyński, Figure Eights, Möbius Bands, and More: Conformation and Aromaticity of Porphyrinoids, *Angew. Chem., Int. Ed.*, 2011, **50**, 4288–4340; (*b*) S. Saito and A. Osuka, Expanded Porphyrins: Intriguing Structures, Electronic Properties, and Reactivities, *Angew. Chem., Int. Ed.*, 2011, **50**, 4342–4373; (*c*) K. Mitsuno, T. Yoshino, I. Gupta, S. Mori, S. Karasawa, M. Ishida and H. Furuta, Doubly N-Confused [36]Octaphyrin(1.1.1.1.1.1.1.1): Isomerization, Bis-Metal Coordination, and Topological Chirality, *Angew. Chem., Int. Ed.*, 2017, **56**, 14252–14256; (*d*) K. Senthilkumar, M. Kondratowicz, T. Lis, P. J. Chmielewski, J. Cybińska, J. L. Zafra, J. Casado, T. Vives, J. Crassous, L. Favereau and M. Stępień, Lemniscular [16]Cycloparaphenylene: A Radially Conjugated Figure-Eight Aromatic Molecule, *J. Am. Chem. Soc.*, 2019, **141**, 7421–7427; (*e*) J. Oniki, T. Moriuchi, K. Kamochi, M. Tobisu and T. Amaya, Linear [3] Spirobifluorenylene: An S-Shaped Molecular Geometry of *p*-Oligophenyls, *J. Am. Chem. Soc.*, 2019, **141**, 18238–18245; (*f*) M. Krzeszewski, H. Ito and K. Itami, Infinitene: A Helically Twisted Figure-Eight [12]Circulene Topoisomer, *J. Am. Chem. Soc.*, 2022, **144**, 862–871; (*g*) J. Malinčík, S. Gaikwad, J. P. Mora-Fuentes, M.-A. Boillat, A. Prescimone, D. Häussinger, A. G. Campaña and T. Šolomek, Circularly Polarized Luminescence in a Möbius Helicene Carbon Nanohoop, *Angew. Chem., Int. Ed.*, 2022, **61**, e202208591; (*h*) R. Yoshina, J. Hirano, E. Nishimoto, Y. Sakamoto, K. Tajima, S. Minabe, M. Uyanik, K. Ishihara, T. Ikai, E. Yashima, T. Omine, F. Ishiwari, A. Saeki, J. Kim, J. Oh, D. Kim, G. Liu, T. Yasuda, H. Shinokubo and N. Fukui, Inner-Bond-Cleavage Approach to Figure-Eight Macrocycles from Planar Aromatic Hydrocarbons, *J. Am. Chem. Soc.*, 2024, **146**, 29383–29390.

22 Double helicate has been developed as a chiral host, see: N. Ousaka, S. Yamamoto, H. Iida, T. Iwata, S. Ito, Y. Hijikata, S. Irle and E. Yashima, Water-Mediated Deracemization of a Bisporphyrin Helicate Assisted by Diastereoselective Encapsulation of Chiral Guests, *Nat. Commun.*, 2019, **10**, 1457.

23 (*a*) D. M. Walba, R. M. Richards and R. C. Haltiwange, Total Synthesis of the First Molecular Möbius Strip, *J. Am. Chem. Soc.*, 1982, **104**, 3219–3221; (*b*) D. M. Walba, J. Simon and F. Harary, Topicity of Vertices and Edges in the Möbius Ladders: A Topological Result with Chemical Implications, *Tetrahedron Lett.*, 1988, **29**, 731–734.

24 Selected reviews of molecular knots, links, and the related compounds: (*a*) O. Lukin and F. Vögtle, Knotting and Threading of Molecules: Chemistry and Chirality of Molecular Knots and Their Assemblies, *Angew. Chem., Int. Ed.*, 2005, **44**, 1456–1477; (*b*) R. S. Forgan, J.-P. Sauvage and J. F. Stoddart, Chemical Topology: Complex Molecular Knots, Links, and Entanglements, *Chem. Rev.*, 2011, **111**, 5434–5464; (*c*) J.-P. Sauvage and D. B. Amabilino, The Beauty of Knots at the Molecular Level, *Top. Curr. Chem.*, 2012, **323**, 107–126; (*d*) S. D. P. Fielden, D. A. Leigh and S. L. Woltering, Molecular Knots, *Angew. Chem., Int. Ed.*, 2017, **56**, 11166–11194; (*e*) W.-X. Gao, H.-J. Feng, B.-B. Guo, Y. Lu and G.-X. Jin, Coordination-Directed Construction of Molecular Links, *Chem. Rev.*, 2020, **120**, 6288–6325; (*f*) T. Sawada and M. Fujita, Folding and Assembly of Metal-Linked Peptidic Nanostructures, *Chem*, 2020, **6**, 1861–1876; (*g*) Z. Ashbridge, S. D. P. Fielden, D. A. Leigh, L. Pirvu, F. Schaufelberger and L. Zhang, Knotting Matters: Orderly Molecular Entanglements, *Chem. Soc. Rev.*, 2022, **51**, 7779–7809.

25 G. Gil-Ramírez, S. Hoekman, M. O. Kitching, D. A. Leigh, I. J. Vitorica-Yrezabal and G. Zhang, Tying a Molecular Overhand Knot of Single Handedness and Asymmetric Catalysis with the Corresponding Pseudo-D_3-Symmetric Trefoil Knot, *J. Am. Chem. Soc.*, 2016, **138**, 13159–13162.

26 H. Fujihara, M. Naito, T. Yashima, Y. Okada, N. Kobayashi, S. Miyagawa, H. Takaya and Y. Tokunaga, Synthesis of Cross-Chain Bridging Cryptands and Induction of Molecular Chirality, *Org. Lett.*, 2023, **25**, 8959–8964.

27 We reported a part of this study as a patent: Y. Tokunaga and M. Naito, Optically Active compound and Method for Producing the Same, Coordination Compound Containing Optically Active Compound, Cyclic Compound, as Well as Intermediate Compounds, JP2021130627A, 2021.
28 The number of oxygen atoms in each bridge is used for the abbreviated nomenclature of this type of cryptand in this paper.
29 The products will be reported elsewhere.
30 O. Trapp, G. Schoetz and V. Schurig, Determination of Enantiomerization Barriers by Dynamic and Stopped-Flow Chromatographic Methods, *Chirality*, 2001, **13**, 403–414.
31 T. Kimura, S. Miyagawa, H. Takaya, M. Naito and Y. Tokunaga, Locking the Dynamic Axial Chirality of Biphenyl Crown Ethers through Threading, *Chem. – Asian J.*, 2020, **15**, 3897–3903.